

Analysis of polarization independent Mach-Zehnder type integrated optical isolator

O. Zhuromskyy, M. Lohmeyer, N. Bahlmann, H. Dötsch, P. Hertel

Universität Osnabrück

A.F. Popkov

Zelenograd Research Institute of Physical Problems, Moscow

Abstract— We propose for the first time an integrated optical isolator independent of light polarization. A Mach-Zehnder interferometer with two nonreciprocal phase shifters, one for TE modes and another one for TM modes can be adjusted so that it blocks the fundamental modes of the waveguides constituting the interferometer propagating in one direction and is transparent for the modes propagating in the opposite direction. If the interferometer branch waveguides are in single mode regime, the performance of the device will not depend on the polarization of incoming light. The nonreciprocal phase shifters can be realized on structures with magnetization tangential to the propagation direction. Three geometries of nonreciprocal phase shifters are discussed and tolerances are estimated.

Keywords— Integrated optics, optical isolators

I. Introduction

MAGNETO-OPTICAL isolators are used in optical communication devices to protect the light source from reflected light causing instability [1] [2] [3] [4] [5]. Currently only bulk isolators are available. There are a couple of papers dealing with integrated optical isolators based on Mach-Zehnder interferometry for incoming light with definite polarization [6] [7] [8]. Here we present a concept of an integrated optical isolator for arbitrary polarized light. The Mach-Zehnder type optical isolator is based on single mode waveguides. One branch operates as a nonreciprocal phase shifter for TE-modes, the other branch introduces a nonreciprocal phase shift for TM-modes. We show that the device can be adjusted so that it blocks light of both polarizations in one direction of propagation while it is transparent for both modes propagating in the opposite direction. It turns out that complete constructive and destructive interference can be achieved only for certain waveguide geometries. The vectorial wave matching method [9] [10] was used to calculate guided modes of the waveguides. Gyrotropy is treated by means of perturbation theory.

II. NONRECIPROCAL PHASE SHIFTERS

Fig.1 shows the magneto optical waveguides investigated in this paper. In configuration (a) the magnetization is adjusted along the normal of the waveguide substrate, and the waveguide is divided by a vertical boundary in two regions with opposite signs of the Faraday rotation. In this regions the gyrotropic contribution to the permittivity

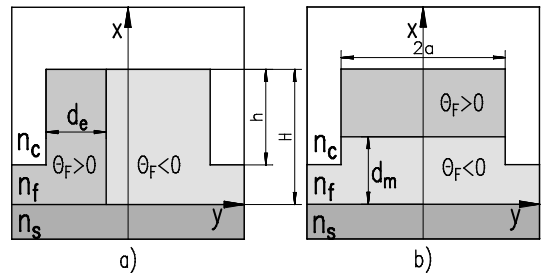


Fig. 1. General geometry of the phase shifters: a) for TE modes with vertical boundary, b) for TM modes with horizontal boundary.

tensor has the form

$$\Delta\epsilon = \begin{pmatrix} 0 & 0 & 0 \\ 0 & 0 & -i\gamma_x \\ 0 & i\gamma_x & 0 \end{pmatrix}. \quad (1)$$

Configuration (b) comprises a double layer waveguide made of materials with opposite signs of the Faraday rotation. The magnetization is adjusted along the y axis and leads to a permittivity contribution

$$\Delta\epsilon = \begin{pmatrix} 0 & 0 & i\gamma_y \\ 0 & 0 & 0 \\ -i\gamma_y & 0 & 0 \end{pmatrix}. \quad (2)$$

The off diagonal entries $\gamma_{x,y}$ are related to the specific Faraday rotation Θ_F and vacuum wavelength λ by $\gamma_{x,y} = n_f \lambda \Theta_F / \pi$. Here n_f is the refractive index of the film.

The electromagnetic fields of the guided modes can be written in the form $\vec{E}(x,y)e^{i(\omega t - \beta z)}$, $\vec{H}(x,y)e^{i(\omega t - \beta z)}$, where ω denotes the angular frequency and β is the mode propagation constant. In the framework of perturbation theory, the shift $\delta\beta$ of a wave number β due to gyrotropy is determined by the expression [11]

$$\delta\beta = \omega\epsilon_0 \frac{\iint \vec{E}^* \Delta\epsilon \vec{E} dx dy}{\iint [\vec{E} \times \vec{H}^* + \vec{E}^* \times \vec{H}]_z dx dy}, \quad (3)$$

where $\Delta\epsilon$ is the part of the permittivity tensor representing gyrotropy. For opposite directions of light propagation the sign of γ is reversed. Thus there is a difference of $2\delta\beta$ between the wavenumbers of forward and backward propagating modes. The cross section of the waveguide can be divided into rectangles with constant permittivity.

Thus, inside the rectangles the Maxwell's divergence equation $\vec{\nabla} \cdot \vec{D} = 0$ has the form $\vec{\nabla} \cdot \vec{E} = 0$. In semi-vectorial approximation we assume $E_x = 0$ and $E_z = i\partial_y E_y / \beta$ for TE modes and $E_y = 0$ and $E_z = i\partial_x E_x / \beta$ for TM modes. We will obtain the phase shift for TE modes in media with the magnetization along the x direction,

$$\delta\beta_{\text{TE}} = \frac{\omega\epsilon_0}{\beta_{\text{TE}}N} \iint \gamma_x E_y^* \partial_y E_y dx dy, \quad (4)$$

and for TM modes in media with the magnetization along the y direction,

$$\delta\beta_{\text{TM}} = -\frac{\omega\epsilon_0}{\beta_{\text{TM}}N} \iint \gamma_y E_x^* \partial_x E_x dx dy, \quad (5)$$

where

$$N = \frac{1}{2} \iint [\vec{E} \times \vec{H}^* + \vec{E}^* \times \vec{H}]_z dx dy.$$

Taking into account the symmetry of the guided TE and TM modes, the largest phase shift will occur in a structure where the boundary separating the regions with opposite signs of the Faraday rotation is placed at the mode field maximum [12] [13].

In section IV below we are interested especially in waveguides with phase matched fundamental TE and TM modes, and gyrotropic polarization conversion can not be excluded a priori. Fortunately, for the geometries discussed here, there is no such effect, as can be shown by symmetry arguments. Due to the symmetry of the structures there occurs no TE-TM conversion in the phase shifters since the coupling coefficients of the fundamental modes vanish. For the structure of Fig.1a the coupling coefficient [14] is proportional to

$$\iint \gamma_x (-E_y^{TE*} E_z^{TM} + E_z^{TE*} E_y^{TM}) dx dy.$$

Integration along the y axis yields zero because γ_x is asymmetrical and the products of fields are symmetrical. The coupling coefficient for the structure of Fig.1b is proportional to

$$\iint \gamma_y (E_x^{TE*} E_z^{TM} - E_z^{TE*} E_x^{TM}) dx dy.$$

This integral also vanishes because γ_y has even symmetry along the y axis and the field products have odd symmetry.

To produce the TM phase shifter, a two layer waveguide should be used [12]. A phase shifter for TE modes may be realized by a vertical compensation wall [15] or domain wall [13] at the center of the rib waveguide. The exact alignment of the magnetization can be achieved by strips of permanent magnets parallel to the rib waveguides of the interferometer. This technique has already been demonstrated by Levy et al. [16].

For our calculations expression (3) was used with fully vectorial hybrid modes. For fully vectorial hybrid modes the configuration of Fig.1a yields a significant phase shift for TE-like modes and a comparatively small phase shift for

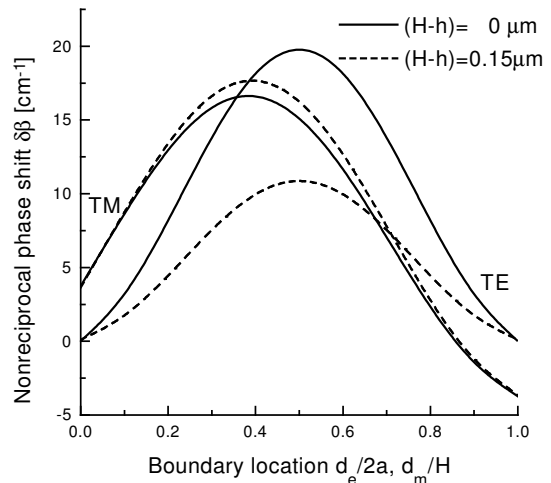


Fig. 2. The dependence of the phase shift $\delta\beta$ on the boundary location $d_e/2a$ and d_m/H (see Fig.1). $H=0.7\mu\text{m}$, $a=0.5\mu\text{m}$, $\lambda=1.3\mu\text{m}$, $n_f=2.2$, $n_s=1.9$, $n_c=1.0$, $\gamma = \pm 0.005$. The solid line corresponds to the structure without lateral film, $H=h$, the dashed line corresponds to the structure with $H-h=0.15\mu\text{m}$.

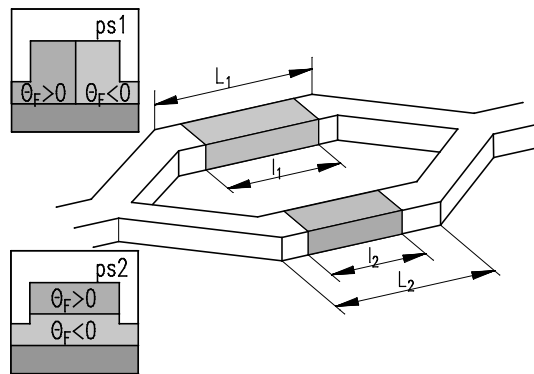


Fig. 3. Mach-Zehnder interferometer with two nonreciprocal phase shifters.

TM-like modes, while the configuration of Fig.1b yields a large phase shift for TM-like modes and a small one for TE-like modes. We can expect the phase shift to be of the same order of magnitude for TE and TM modes in the waveguides with vertical and horizontal boundaries, respectively. The dependence of the phase shift of TE and TM modes on the boundary location is depicted in Fig.2. The maximum phase shift for TM modes is observed for a boundary location $d_m/H \sim 0.4$ since the structure is asymmetrical along the x axis. In the rib waveguides ($H > h$) the TE phase shift becomes smaller because the TE mode spreads wider.

III. INTERFEROMETER

Consider the structure with two nonreciprocal shifters depicted in Fig.3. The shifter for TE mode is embedded into branch 1 and for TM mode into branch 2. If the intrinsic phase difference of the branches without gyrotropy is $\pi/2$ and the phase difference of the shifters for the light propagating in forward direction is $-\pi/2$ the total phase difference is zero and the light interferes constructively. For

the light propagating in backward direction the phase difference of the shifters is $\pi/2$, the total phase difference is π and the light interferes destructively. The phase matching conditions for both TE and TM modes constitute the following system of equations

$$\begin{aligned} L_1\beta_{\text{TE}}^1 - L_2\beta_{\text{TE}}^2 &= \pi/2 + \pi n, \\ L_1\beta_{\text{TM}}^1 - L_2\beta_{\text{TM}}^2 &= \pi/2 + \pi m, \\ l_1\delta\beta_{\text{TE}}^1 - l_2\delta\beta_{\text{TE}}^2 &= \pi/2 + 2\pi p, \\ l_1\delta\beta_{\text{TM}}^1 - l_2\delta\beta_{\text{TM}}^2 &= (-1)^{n-m}\pi/2 + 2\pi q. \end{aligned} \quad (6)$$

Here $\beta_{\text{TE,TM}}^{1,2}$ are the wavenumbers of TE and TM modes in branches 1 and 2 without magnetization, $\delta\beta_{\text{TE,TM}}^{1,2}$ are the wavenumber shifts due to gyrotropy, $L_{1,2}$ are the lengths of interferometer branches, $l_{1,2}$ are the lengths of the shifters and n, m, p, q are integers.

The first pair of the system equations determines the interferometer branch lengths, the second determines the shifter lengths. For the sake of convenience the first and the second pairs of equations will be discussed separately. The system assumes equality of light power in both branches. To achieve 3dB splitting in Y-junction, the geometries of the interferometer branches (besides lengths) are to be the same. This leads to the equality of wavenumbers in the two branches,

$$\beta_{\text{TE}}^1 = \beta_{\text{TE}}^2 \text{ and } \beta_{\text{TM}}^1 = \beta_{\text{TM}}^2.$$

Now the equations for the interferometer branch lengths read

$$\begin{aligned} \beta_{\text{TE}}(L_1 - L_2) &= \pi/2 + \pi n, \\ \beta_{\text{TM}}(L_1 - L_2) &= \pi/2 + \pi m. \end{aligned} \quad (7)$$

System (7) has solutions only for certain geometries where

$$\frac{\beta_{\text{TE}}}{\beta_{\text{TM}}} = \frac{1 + 2n}{1 + 2m}. \quad (8)$$

With conditions (8) satisfied, system (7) reduces to a single equation and the branch length difference is

$$L_1 - L_2 = \frac{\pi}{2\beta_{\text{TE}}}(1 + 2n), \quad (9)$$

while the total length of the interferometer is determined by the shifter lengths and the length of the Y-junctions. To obtain the lengths of the shifters, the following equations are to be solved

$$\begin{aligned} l_1\delta\beta_{\text{TE}}^1 - l_2\delta\beta_{\text{TE}}^2 &= \pi/2 + 2\pi p, \\ l_1\delta\beta_{\text{TM}}^1 - l_2\delta\beta_{\text{TM}}^2 &= (-1)^{n-m}\pi/2 + 2\pi q. \end{aligned} \quad (10)$$

In semi vectorial approximation the terms $\delta\beta_{\text{TM}}^1$ and $\delta\beta_{\text{TE}}^2$ in (10) vanish. For vectorial modes, components E_y^{TM} and E_x^{TE} exist and the terms cannot be neglected. The length of the Y-junction is strongly affected by the asymmetry of the interferometer, and since the real materials are lossy, a large difference of the interferometer branches will lead to incomplete destructive interference. Therefore the asymmetry of the interferometer must be as small as possible. Since β_{TE} and β_{TM} are close to each other, it is impossible

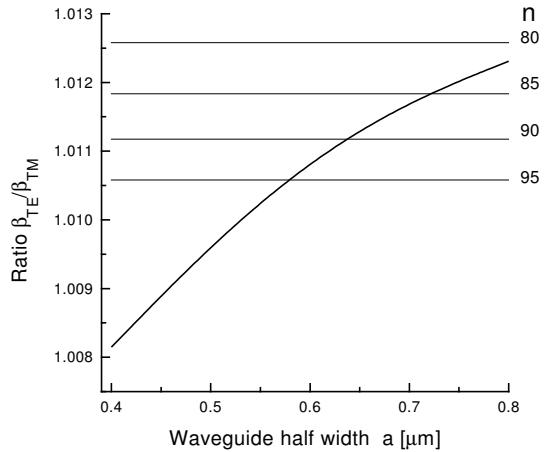


Fig. 4. The ratio $\beta_{\text{TE}}/\beta_{\text{TM}}$ versus the waveguide half width a . The parameters are presented in Table(I) column I; the horizontal lines correspond to the ratio given by Eq.(11) with n denoted in the figure.

to choose n arbitrarily small. The ratio on the right side of the expression (8), for the case $n > m$, is minimal when $m = n - 1$. In this case the following conditions for the wavenumber β_{TE} and β_{TM} are to be satisfied

$$\frac{\beta_{\text{TE}}}{\beta_{\text{TM}}} = \frac{2n + 1}{2n - 1}. \quad (11)$$

The ratio of the right hand side of (11) is proportional to $\sim 1 + 1/(n - 1/2)$. A smaller ratio $\beta_{\text{TE}}/\beta_{\text{TM}}$ results in a large interferometer branch difference. When $\beta_{\text{TE}} = \beta_{\text{TM}}$, the branch length difference has discrete values with step π/β_{TE} and minimum value $\pi/2\beta_{\text{TE}}$.

IV. INTERFEROMETER PARAMETERS

The mode field distribution and the relation between the wavenumbers of TE and TM modes are strongly dependent on waveguide geometry. In this section we will examine some peculiarities of the isolators with different waveguide structures. Also we determine the parameters of the waveguides to obtain the shortest nonreciprocal elements possible.

A. Rib waveguides

Consider the interferometer with nonreciprocal phase shifters based on the rib waveguide of Fig.1. The dependence of the ratio $\beta_{\text{TE}}/\beta_{\text{TM}}$ on the waveguide half width a is presented in Fig.4. The horizontal lines correspond to the ratio in the right hand side part of (11) with values of n indicated in the figure. The parameters corresponding to intersections are suitable for the isolator. With $n = 85$, the difference of the interferometer branches calculated with (9) is $\approx 30\mu\text{m}$. For narrower ribs larger values of n are required to match condition (11). The maximum of the waveguide width is restricted to the range below $1.1\mu\text{m}$ to keep the waveguide monomode. The possible parameters of the isolator are presented in Table(I) column I.

TABLE I

The possible parameters for the polarization independent integrated optical isolator: I - rib wave- guide; II - square embedded waveguide; III - raised strip waveguide.

	I	II	III
n_f	2.2	2.2	2.2
n_s	1.9	1.9	1.9
n_c	1.0	1.9	1.0
$\gamma_{x,y}$	± 0.005	± 0.005	± 0.005
λ	$1.3 \mu\text{m}$	$1.3 \mu\text{m}$	$1.3 \mu\text{m}$
H	$0.7 \mu\text{m}$	$0.9 \mu\text{m}$	$0.76 \mu\text{m}$
h	$0.4 \mu\text{m}$	$0.9 \mu\text{m}$	$0.76 \mu\text{m}$
a	$0.705 \mu\text{m}$	$0.45 \mu\text{m}$	$0.477 \mu\text{m}$
$L_1 - L_2$	$26.903 \mu\text{m}$	$0.158 \mu\text{m}$	$0.161 \mu\text{m}$
l_1	1.325 mm	1.389 mm	0.774 mm
l_2	1.103 mm	1.389 mm	0.881 mm

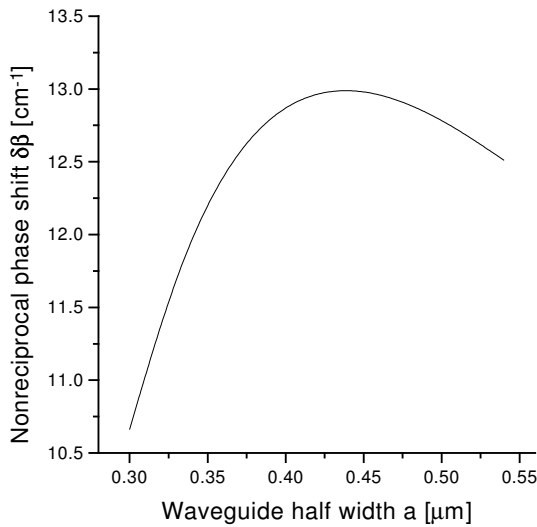


Fig. 5. Phase shift in the square embedded waveguide versus waveguide half width a ; $n_f=2.2$, $n_c=1.9$, $\gamma = \pm 0.005$ and $\lambda = 1.3\mu\text{m}$.

B. Square embedded waveguide

The simplest structure where the condition (8) is satisfied for equal m and n is a square embedded waveguide with $H = 2a$, $H - h = 0$ and $n_c = n_s$, see Fig.1. Due to the symmetry of the structure we obtain $\beta_{TE} = \beta_{TM}$ and $\delta\beta_{TE}^{a,b} = \delta\beta_{TM}^{b,a}$ where superscripts a and b refer to the phase shifter geometries of Fig.1. The dependence of the wavenumber shift $\delta\beta$ on waveguide half width a is depicted in Fig.5. The possible parameters of the structure for the point near the maximum of $\delta\beta$ are presented in Table(I) column II. The disadvantage of the square embedded waveguide is that it is difficult to tune it after manufacturing.

C. Raised strip waveguide

A raised strip waveguide is a waveguide without a film on the sides of the rib, $H - h = 0$ (Fig.1). It is possible to adjust the waveguide height and width such that the wavenumbers of TE and TM modes are equal, $\beta_{TE} = \beta_{TM}$.

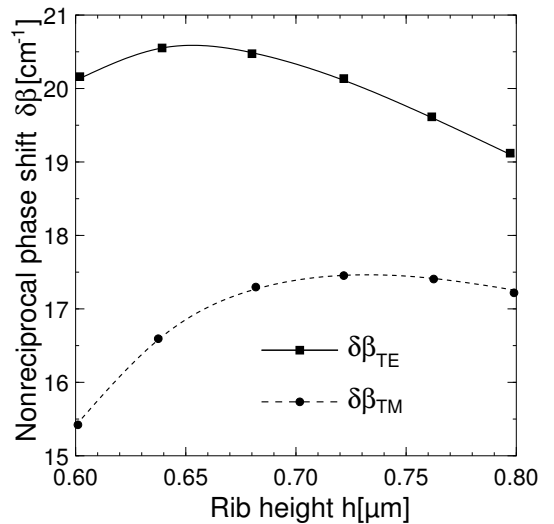


Fig. 6. The phase shift for raised strip waveguides with equal wavenumbers $\beta_{TE} = \beta_{TM}$, squares - TE mode, circles - TM mode; $n_f = 2.2$, $n_s = 1.9$, $n_c = 1.0$, $\gamma = \pm 0.005$, $\lambda = 1.3\mu\text{m}$.

The dependence of the wavenumber shift $\delta\beta$ is shown in Fig.6. Each point on the plot corresponds to the waveguide geometry with equal TE and TM mode wavenumbers. The possible parameters of the structure corresponding to the maximum of $\delta\beta_{TM}$ are presented in Table(I) column III.

V. TOLERANCES

The output power P_{out} of the isolator can be calculated with the relation [17]

$$P_{\text{out}} = \frac{P_{\text{in}}}{2}(1 + \cos(\phi_1 - \phi_2)), \quad (12)$$

where ϕ_1 and ϕ_2 are phase changes of the light propagating through the first and the second branches of the isolator. The performance of the device is determined by the output powers P_{forw} and P_{back} of the light propagating in forward and backward direction and is defined by the expression

$$\text{IS} = 10 \log_{10} \frac{P_{\text{back}}}{P_{\text{forw}}}. \quad (13)$$

The influence of variations of the structure parameters on the isolator performance is calculated with the assumption that all the other parameters have their optimal value.

The limitations on the interferometer fabrication tolerances are rather strict, see Figs.7, 8. The only way to adjust the intrinsic phase shifts of the interferometer is post fabrication tuning [18]. The influence of the deviation of the interferometer branch geometries on the gyrotropic phase shift is assumed to be of higher perturbation order and will thus be neglected. Fabrication of the nonreciprocal phase shifters does not require such small tolerances. The length of the shifters is not a critical parameter, Fig.9. To achieve better than 30dB isolation the boundaries dividing the regions with opposite sign of Faraday rotation can deviate by $0.01\mu\text{m}$ from their optimal location, Fig.10.

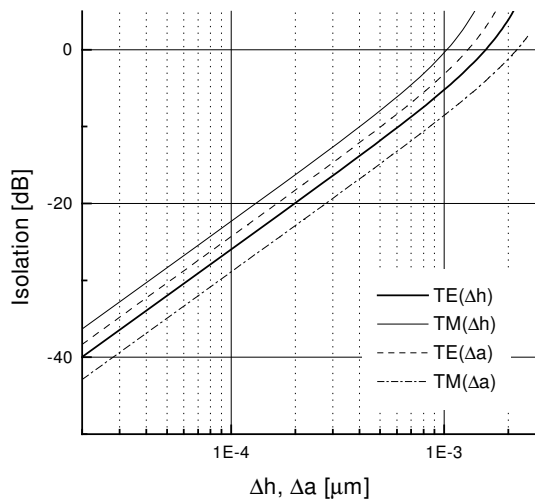


Fig. 7. The dependence of interferometer isolation on deviation of waveguide geometry parameters a and h for the structure in column III Table I.

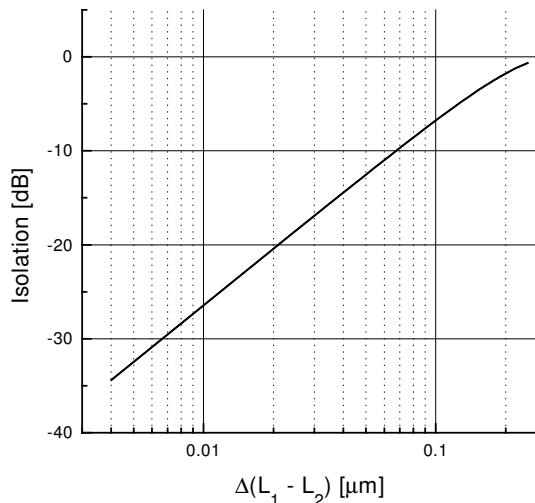


Fig. 8. The dependence of interferometer isolation on deviation of interferometer parameters $L_1 - L_2$ for the structure in column III Table I.

Furthermore, the performance of the isolator may be affected by optical losses. Usually, the damping of the TM mode is larger than that of the TE mode. This effect is probably caused by the roughness of the rib flanks induced by the waveguide preparation [19]. A difference of TE and TM mode losses does not affect the isolation, it will only influence the forward loss of the isolator. Due to the different lengths of the interferometer arms, the interference will not be complete if losses are taken into account. However, a difference of $30\mu\text{m}$ in length induces a difference of the light intensities the interferometer arms of $\sim 3 \cdot 10^{-3}\text{dB}$ for a damping of 1dB/cm . This effect can be neglected.

VI. CONCLUSIONS

The first concept of an integrated optical isolator for light of arbitrary polarization is presented. The basis of the isolator is a Mach-Zehnder interferometer with nonreciprocal

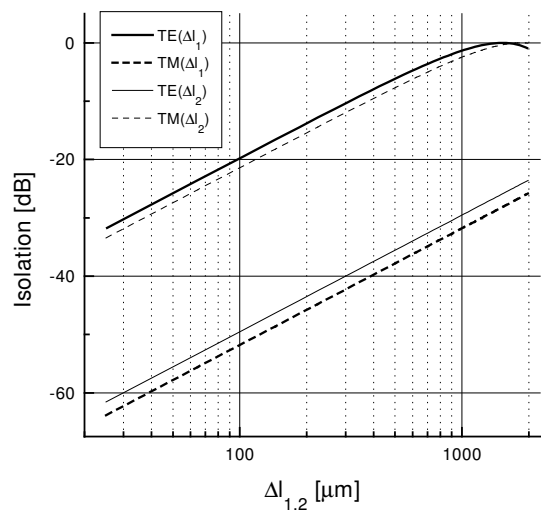


Fig. 9. The dependence of interferometer isolation on deviation of nonreciprocal phase shifter lengths l_1 and l_2 for the structure in column III Table I.

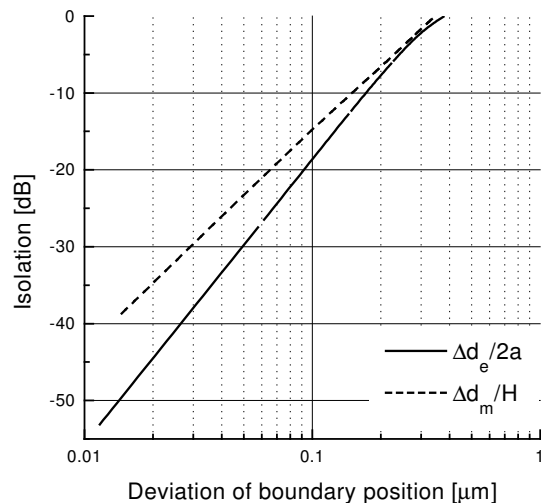


Fig. 10. The dependence of interferometer isolation on the deviation of boundary location $d_e/2a$ for TE mode and d_m/H for TM mode for the structure described in Table I, column III.

phase shifters for TE and TM polarized light. The most promising geometry for the device is the raised strip waveguide with equal wavenumbers for zero order TE and TM modes. Its interferometer branch length difference is small if compared with the rib waveguide. The gyrotropic phase shifts for TE and TM modes are almost equal. In the rib waveguide the existence of the film on the sides of the rib causes the penetration of the TE mode into the substrate. This results in lower phase shift and large shifter length. The strict fabrication requirements for the waveguide geometries and the interferometer require post fabrication tuning which is difficult with the embedded waveguide.

REFERENCES

- [1] R. Wolfe, JR. Dillon, R. A. Liberman, and V. J. Fratello, "Broadband magneto-optic waveguide isolator," *Applied Physics Letters*, vol. 57, no. 10, pp. 960-962, 1990.
- [2] K. Ando, T. Okoshi, and N. Koshizuka, "Waveguide magneto-

- optics isolator fabricated by laser annealing," *Applied Physics Letters*, vol. 53, no. 1, pp. 4–6, 1988.
- [3] H. Hemme, H. Dötsch, and P. Hertel, "Integrated optical isolator based on nonreciprocal-mode cut-off," *Applied Optics*, vol. 29, no. 18, pp. 2741–2744, 1990.
 - [4] S. Yamamoto, Y. Okamura, and T. Makimoto, "Analysis and design of semileaky-type thin-film optical waveguide isolator," *IEEE Journal of Quantum Electronics*, vol. 12, no. 12, pp. 764–770, 1976.
 - [5] T. Shintaku, "Integrated optical isolator based on nonreciprocal higher order mode conversion," *Applied Physics Letters*, vol. 66, no. 21, pp. 2789–2791, 1995.
 - [6] F. Auracher and H. Witte, "A new design for an integrated optical isolator," *Optical Communication*, vol. 13, no. 4, pp. 435–438, 1975.
 - [7] Y. Okamura, T. Negami, and S. Yamamoto, "Integrated optical isolator and circulator using nonreciprocal phase shifters: a proposal," *Applied Optics*, vol. 23, no. 11, pp. 1886–1889, 1984.
 - [8] N. Bahlmann, M. Lohmeyer, M. Wallenhorst, H. Dötsch, and P. Hertel, "An improved design for an integrated optical isolator based on nonreciprocal Mach-Zehnder interferometry," *Optical and Quantum Electronics; special issue on: Optical Waveguide Theory and Numerical Modeling*, 1998, to be published.
 - [9] M. Lohmeyer, "Wave-matching method for mode analysis of dielectric waveguides," *Optical and Quantum Electronics*, vol. 29, pp. 907–922, 1997.
 - [10] M. Lohmeyer, "Vectorial wave-matching mode analysis of integrated optical waveguides," *Optical and Quantum Electronics*, 1998, accepted for publication.
 - [11] G. J. Gabriel and M. E. Brodwin, "The solution of guided waves in inhomogeneous anisotropic media by perturbation and variational methods," *IEEE Transactions on Microwave Theory and Techniques*, vol. 13, no. 3, pp. 364–370, 1965.
 - [12] M. Wallenhorst, M. Niemöller, H. Dötsch, P. Hertel, R. Gerhardt, and B. Gather, "Enhancement of the nonreciprocal magneto-optic effect of TM modes using iron garnet double layers with opposite Faraday rotation," *Journal of Applied Physics*, vol. 77, no. 7, pp. 2902–2905, 1995.
 - [13] A. F. Popkov, M. Fehndrich, M. Lohmeyer, and H. Dötsch, "Nonreciprocal TE-mode phase shift by domain walls in magneto-optic rib waveguides," *Applied Physics Letters*, vol. 72, no. 20, pp. 2508–2510, 1998.
 - [14] S. Yamamoto, Y. Koyamoda, and T. Makimoto, "Normal - mode analysis of anisotropic and gyrotropic thin - film waveguides for integrated optics," *Journal of Applied Physics*, vol. 43, no. 12, pp. 5090–5097, 1972.
 - [15] N. Bahlmann, M. Lohmeyer, H. Dötsch, and P. Hertel, "Finite element analysis of nonreciprocal phase shift for TE-modes in magneto-optics rib-waveguides with a compensation wall," *IEEE Journal of Quantum Electronics*, 1998, accepted for publication.
 - [16] M. Levy, R. M. Osgood, Jr. H. Hegde, F. J. Cadieu, R. Wolfe, and V. J. Fratello, "Integrated optical isolators with sputter-deposited thin-film magnets," *IEEE Photonics Technology Letters*, vol. 8, no. 7, pp. 903–905, 1996.
 - [17] W. Karthe and R. Müller, *Integrierte Optik*, Akademische Verlagsgesellschaft Geest & Portig K.-G., Leipzig, 1991.
 - [18] M. J. Ahmed and L. Young, "Mach-Zehnder interferometer tuning with Ta₂O₅ film loading," *Applied Optics*, vol. 22, no. 24, pp. 4082–4087, 1983.
 - [19] R. C. Hewson-Browne, P. C. Kendall, and D. A. Quinney, "Roughness scattering into substrate radiation modes of rib waveguides," *IEE Proceedings*, vol. 136, no. 5, pp. 281–286, 1989, Pt. J.